Available online at www.sciencedirect.com

SciVerse ScienceDirect

Physics Procedia 37 (2012) 2015 – 2022

Physics Procedia

TIPP 2011 - Technology and Instrumentation in Particle Physics 2011

Detector Backgrounds at Muon Colliders[#]

N.V. Mokhov *, S.I. Striganov

Fermilab, Batavia, IL 60510, USA

Abstract

The physics goals of a Muon Collider (MC) can only be achieved with appropriate, self-consistent designs of the ring, interaction region (IR), high-field superconducting magnets, machine-detector interface (MDI) and detector. Recent results from realistically-implemented simulation studies are presented here for a 1.5-TeV MC. It is shown that if the IR and MDI are designed with appropriate shielding, background rates are significantly suppressed in the MC detector. The main characteristics of these backgrounds are also presented.

Keywords: Muon collider; backgrounds; Monte Carlo; MARS15

1. Introduction

The Muon Collider (MC) detector performance is strongly dependent on the rate of background particles striking the various sub-detectors. The deleterious impact of the background and radiation environment produced by muon decays is one of the fundamental and critical issues in determining the feasibility of the MC storage ring, specifically the Interaction Region (IR), Machine-Detector Interface (MDI) and detector. Although incoherent e^+e^- pair production at the Interaction Point (IP) and beam loss on limiting apertures can result in noticeable background levels, muon decays have been identified as the major source of detector backgrounds at a MC [1-3]. The decay length for a 0.75-TeV muon is $\lambda_D = 4.7\times10^6$ m. With 2×10^{12} muons in a bunch, one has 4.28×10^5 decays per meter of the lattice in a single

---

[#] Work supported by Fermi Research Alliance, LLC under contract No. DE-AC02-07CH11359 with the U.S. Department of Energy.

* *E-mail address*: mokhov@fnal.gov.

doi:10.1016/j.phpro.2012.03.761

pass. The MC ring considered here is designed [4, 5] for 1000-turn stores with 15 stores per second. This results in 1.28×10^{10} decays per meter per second for two 0.75-TeV muon beams.

Electrons from muon decays have a mean energy of approximately 1/3 that of the muons. At 0.75 TeV, these ~250-GeV electrons, generated at the above rate, travel to the inside of the ring magnets, and radiate energetic synchrotron photons tangent to the electron trajectory. Electromagnetic showers induced by these electrons and photons in the collider components generate intense fluxes of muons, hadrons and daughter electrons and photons, which create high background and radiation levels both in a detector and in the storage ring at the rate of 0.5-1 kW/m. This is to be compared to the acceptable limit of a few W/m at superconducting (SC) hadron colliders.

Backgrounds – if not suppressed - affect detector performance in three ways: detector component radiation aging and damage, difficulties with reconstruction of objects (e.g., tracks) not related to products of $\mu^+\mu^-$ collisions, and deterioration of detector resolution (e.g., jet energy resolution due to extra energy from background hits).

2. Earlier Findings and New Studies

In very early MC studies, it was found that [1-4]:

- Photon, electron and neutron fluxes and energy deposition in detector components are well beyond technological capabilities if one applies no measures to bring these levels down.
- Tungsten nozzles, starting a few centimeters from IP with ±20-deg outer angle, are the most effective way (~1/500) of background suppression [1, 2]. These nozzles can also fully confine incoherent pairs if the magnetic field of the detector solenoid is $B_{detector} > 3$ T.
- High-field SC dipoles implemented in the final focus region, interlaced with quadrupoles and tungsten shields, provide further reduction of backgrounds.
- With such an IR design, the major source of backgrounds in a MC detector is muon decays in the region confined to about ±25 m from the IP.
- Time gates promise substantial mitigation of background problem in a MC detector (quantified below in section 4.5).

These findings have recently been confirmed and the MC background problems further attacked in coherent studies by collider lattice and magnet designers, particle production and transport experts and detector groups [5, 6]. A consistent design now exists for a compact 0.75×0.75 TeV $\mu^+\mu^-$ collider ring, IR, MDI and chromatic correction section with large momentum acceptance and dynamic aperture, all based on high-field Nb_3Sn SC magnets adequately protected against dynamic heat loads.

3. MARS Modeling of Backgrounds

Energy deposition and detector backgrounds are simulated with the MARS15 code [7]. Realistic details of geometry, materials and magnetic fields are incorporated in the model for a ±200-m region relative to the IP including lattice elements and tunnel, detector components [8], experimental hall and MDI as shown in Fig. 1 (the y-axis points out of the page). To protect the SC magnets and detector, 10 and 20-cm long tungsten shields with 5 $\sigma_{x,y}$ elliptical apertures are inserted between the SC IR magnets to protect the coils.

Details of MDI are shown in Fig. 2 (left) with tungsten nozzles seen in yellow. The parameters of the nozzles were carefully optimized [5] to minimize background particle fluxes entering the detector sensitive volumes without significantly impacting the detector performance in the forward direction. The optimized nozzle parameters for the 0.75-TeV muon beams are shown in Fig. 2 (right). The nozzle tips are at ±6 cm from IP with a 0.5-cm initial radius at that location. The nozzle tapers down to a minimal aperture of 0.3-cm radius at z=±100 cm, then re-opens to 1.78 cm at z=±600 cm. The outer angle subtended by the nozzle in the region closest to IP (6 to 100 cm) is the most critical parameter: the larger this angle the better background suppression, however the impact on the detector performance, especially in the forward region, becomes higher. Presently this angle is 10 degrees (to be compared with an earlier 20-degree value). The angle is then decreased to 5 degrees at 100 < |z| < 600 cm where the tungsten is encapsulated in a borated polyethylene shell to reduce the flux of low-energy neutrons reflecting and crossing the central detector void.

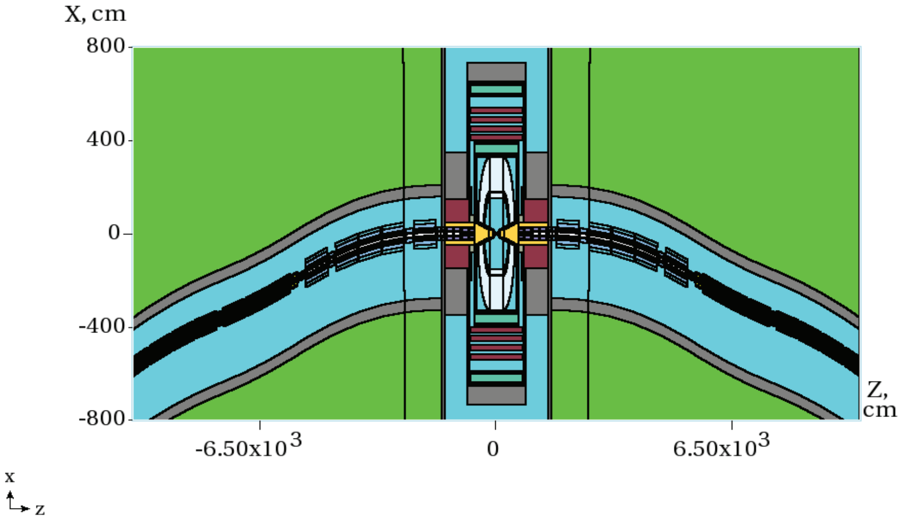

Fig. 1. Plan view of MARS model for IR at |z|<10000 cm).

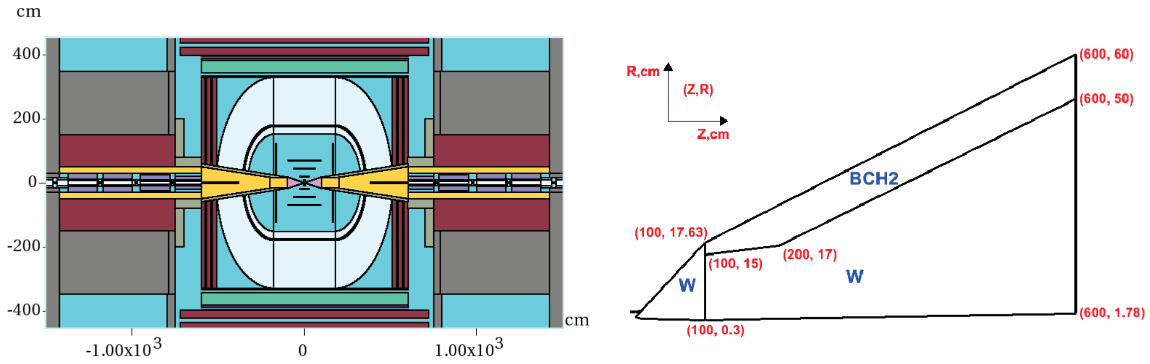

Fig. 2. Details of MDI at |x|<500 cm and |z|<1500 cm (left) and tungsten nozzle (right)

The muon beams are assumed to be aborted after 1000 turns. The particle tracking used cut-off energies E_{th} for this initial study chosen to adequately understand the main features of the background balancing accuracy (E_{th} low) against CPU time (E_{th} high). The minimal cut-off energies in this study range from 0.001 eV for neutrons to 1 MeV for muons and charged hadrons. The cut-off energy in the tunnel concrete walls and soil outside is position-dependent and can be as high as a few GeV at 50-100 m from the IP compared to the above minimal value required in the vicinity of the detector.

Fig. 3 (left) shows muon flux isocontours in the MC IR. These muons – with energies of tens to hundreds of GeV - illuminate the entire detector. They are produced in the Bethe-Heitler process by energetic photons from electromagnetic showers generated by decay electrons in the lattice components. The neutron isofluences inside the detector are shown in Fig. 3 (right). The maximum neutron fluence and absorbed doses in the innermost layer of the silicon tracker (r=3.3 cm) for a one-year operation are at a 10% level of that expected in the LHC detectors at r=4 cm at the nominal luminosity.

The dipoles close to IP and tungsten masks in each interconnect region help reduce background particle fluxes in the detector by a substantial factor. The tungsten nozzles, assisted by the detector solenoid field, trap most of the decay electrons created close to IP as well as most of incoherent e^+e^- pairs generated in the IP. The total numbers of photons and electrons entering the detector per bunch crossing are 1.5×10^{11} and 1.4×10^{9}, respectively, for the minimal studied outer angle of the nozzle of 0.6 degrees, and reduced by three orders of magnitude for the MDI with the angle of 10 degrees as shown in Fig. 2 (right).

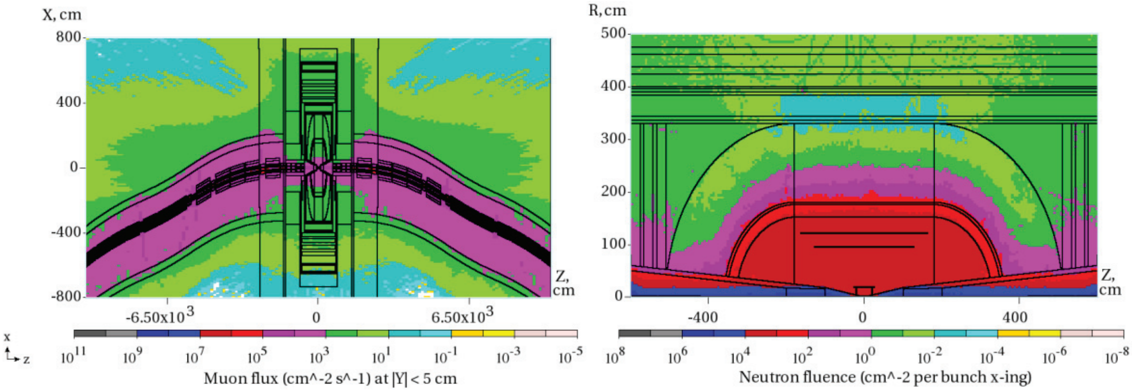

Fig. 3. Muon isoflux in IR orbit plane (left) and azimuthally-averaged neutron isofluence in the detector (right).

In the MARS15 runs, a source term for detector simulations is calculated for all particles entering the detector through the MDI surface. This surface is defined around IP (r=2.2 cm z=±13 cm), on the outer surface of the nozzle up to z=±600 cm, and on the inside of the detector at r=655 cm z=±750 cm. Corresponding high-statistics files have been generated for two 0.75-TeV muon beams, with minimal variation of particle weights, and with full information on the particle origin. The main characteristics of this source term are described in the next section (for cut-off energies indicated in Table 1).

4. Main Characteristics of Backgrounds

4.1. Origin in lattice

As found in earlier studies and confirmed with the current IR and MDI designs, the origin of all particles (except muons) entering the detector is the straight section of about ±25 m near the IP. The combined effect of angular divergence of secondary particles, strong magnetic field of dipoles in IR and tight tungsten masks in interconnect regions is that there is practically no contribution to non-muon detector backgrounds from distances |z| > 25 m (see Fig. 4, left). Excellent performance of the optimized nozzles and MDI shielding along with confinement of decay electrons in the aperture (forcing them to hit the nozzle on the opposite side of IP) result in the longitudinal distributions of particle origins shown in Fig. 3 (left), with a broad maximum from 6 m to 17 m (IP side of the first dipole).

On the contrary, Bethe-Heitler muons hitting the detector are created in the lattice as far as 200 m from IP, with 90% of them produced at ±100 m around IP (Fig. 4, right). As for all other particles, the fine structure of these distributions is related to the lattice details, with pronounced peaks always connected to the high-field SC dipole locations.

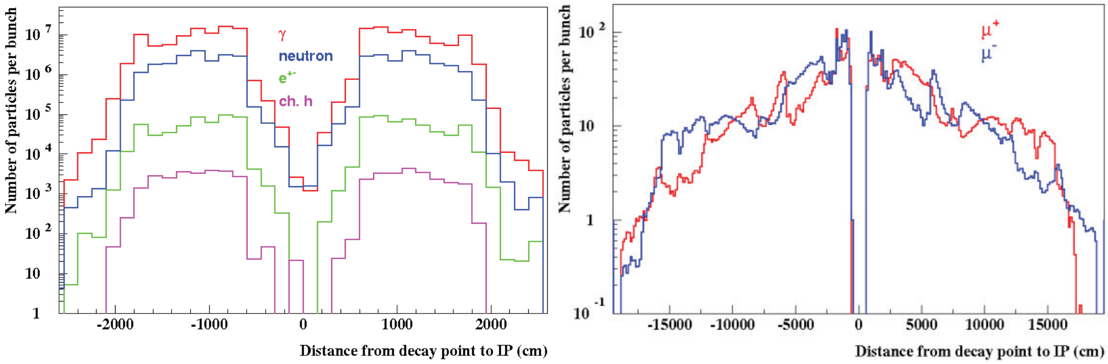

Fig. 4. Numbers of background particles (per bunch crossing) entering the detector as a function of distance along the IR lattice to their production point: Bethe-Heitler muons (right) and other particles (left).

4.2. Spatial distributions at interface surface

Fig. 5 shows longitudinal point-of-entry distributions of backgrounds for a μ^+ beam. Most particles enter the detector through the nozzle outer surface. The maximum yield of photons and electrons is very close to the IP where the shielding is minimal. Neutron and charged hadron yields peak at z = ±1 m. Muons enter the detector through the z = ±750 cm plane (70%) and the nozzle (30%).

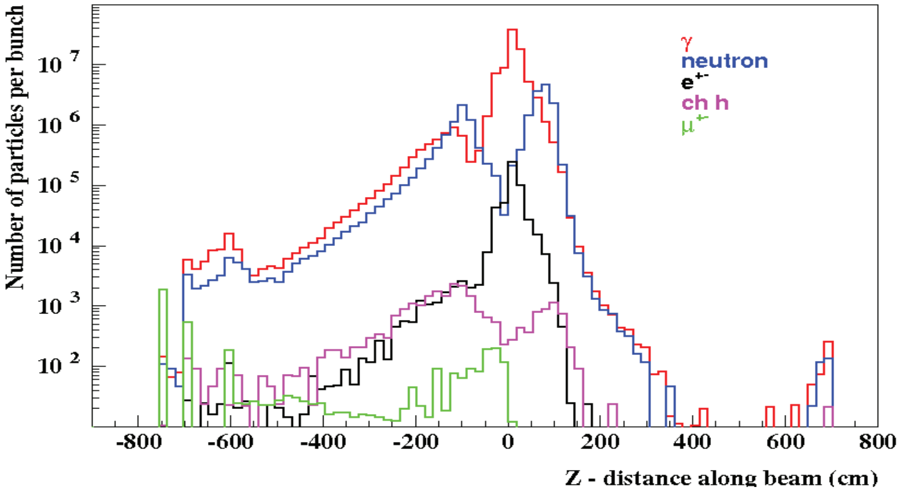

Fig. 5. Longitudinal distributions of entry points of background particles (per bunch crossing) for μ^+ beam moving from the left.

The fact that most particles (except muons) are produced close to the IP and are not affected by the strong dipole magnetic field results in the azimuthal symmetry of the source term with the corresponding distributions at MDI being flat. Angular distributions of these particles on the interface surface also have the azimuthal symmetry. On the contrary, Bethe-Heitler muons are strongly affected by the magnetic fields of the dipoles on their long way to IP. As a result, azimuthal distributions of these muons have a strong asymmetry as shown in Fig. 6 for the μ^+ beam. Secondary positive muons are deflected by the IR element magnetic fields to the same side as a positive muon bunch (negative horizontal direction). Negative muons are deflected to the opposite side. Note, that many muons hit the detector at large radii.

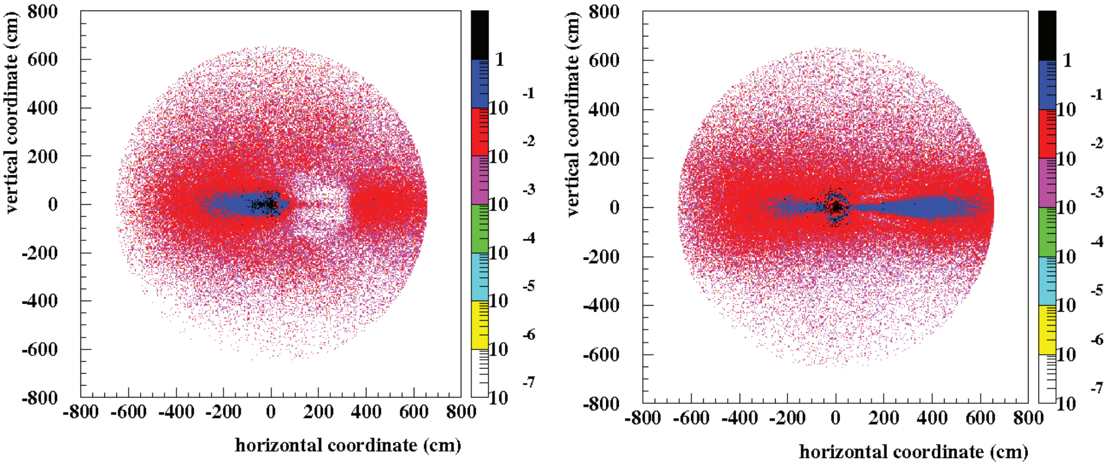

Fig. 6. μ^+ (left) and μ^- (right) distributions at the detector entrance for the μ^+ beam .

4.3. Particle and energy flows into detector

The total numbers of particles (with cut-off energies E_{th} indicated) entering the detector through the MDI surface are given in Table 1 along with particle mean momenta and energy flow. Soft photons and neutrons are the major components. They are followed by electrons and positrons. Mean momenta are rather low except for charged hadrons (~0.5 GeV/c) and Bethe-Heitler muons (22 GeV/c). About 540 TeV of energy is brought to the detector by background particles per bunch crossing. Photons, neutrons and muons contribute about one third each to the energy flow, with two other components being small.

Table 1. Mean numbers <n>, momenta <p> and total kinetic energy flow <EF> of background particles per bunch crossing

Particle (E_{th}, MeV)	<n>	<p>, MeV/c	<EF>, TeV
Photon (0.2)	1.8×10^{8}	0.91	164
Neutron (0.1)	4.1×10^{7}	45	172
Electron/positron (0.2)	1.0×10^{6}	6.0	5.8
Charged hadron (1)	4.8×10^{4}	513	12
Muon (1)	8.0×10^{3}	23030	184

4.4. Momentum spectra

As one can see from Fig. 7, the momentum spread of particles entering the detector through the MDI surface is quite broad. With the kinetic cut-off energies indicated above, photons and electrons with their ~MeV/c mean momenta, have always $p < 0.2$ GeV/c. Hadron momentum reaches ~3 GeV/c, with very different mean values for neutrons and charged hadrons (see Table 1). Bethe-Heitler muons, illuminating the detector, do have the highest momenta of up to 200 GeV/c.

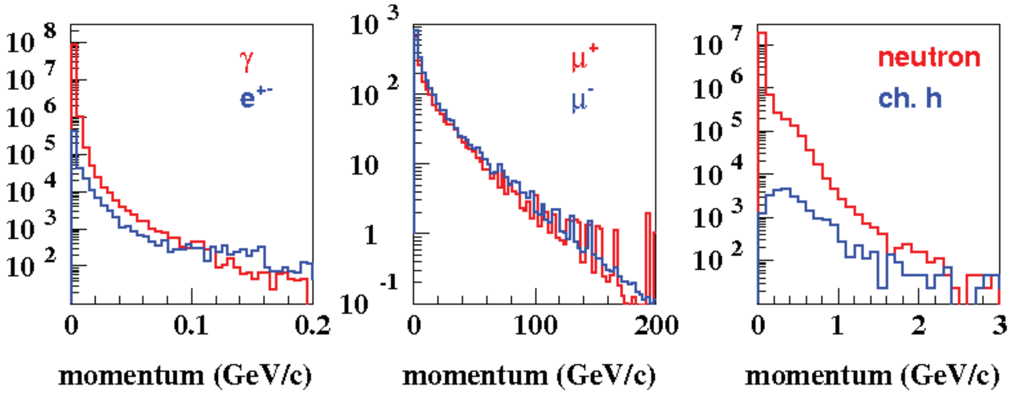

Fig 7. Momentum spectra at MDI for photons and electrons (left), muons (middle) and hadrons (right).

4.5. Time distributions

The time of flight (TOF) of background particles at the MDI surface has a significant spread with respect to the bunch crossing as shown in Fig. 8. Two regions are clearly seen in the TOF distributions. The first one at TOF < 40 ns is related to the direct contributions from particles generated by muon beam decays in the ±17 m region not shielded by the strong magnetic field of the first dipole (see Fig. 4). The long tails for photons, electrons/positrons and neutrons are due to their bouncing and multiple interactions in MDI components at low energies. The long tail for energetic Bethe-Heitler muons is associated with their production at large distances from IP (Fig. 4, right). These properties of the TOF distribution of the source term at MDI suggest that one can use timing in the detector to reduce the number of the readout background hits. As shown in Ref. [9], the background neutron hit rate registered in the vertex and tracking silicon detectors can be reduced by a factor of several hundred by using the 7-ns time window.

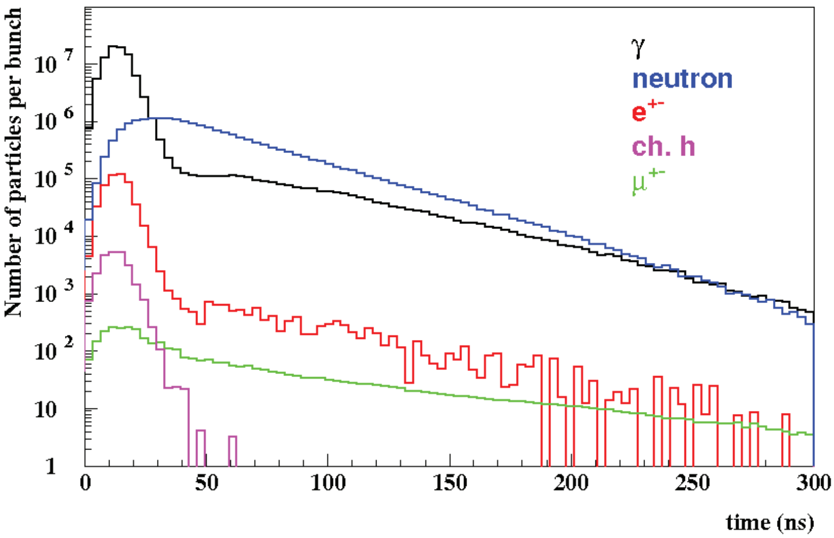

Fig. 8. TOF distributions of background particles at the detector entrance with respect to bunch crossing.

5. Conclusions

The recent developments in the design of the 1.5-TeV center-of-mass Muon Collider ring and interaction region (based on 8-10 T Nb_3Sn SC magnets) along with substantial efforts in Monte-Carlo code developments and optimization studies of the machine-detector interface and appropriate detector technologies assure one that the severe background environment at such a challenging machine can be reduced to tolerable levels. The main characteristics of particle backgrounds entering the collider detector are studied in great details. A good understanding of background properties suggests the ways for suppression of the detector response to the non-IP related hits. We would like to thank Y.I. Alexahin, V.Y. Alexakhin, V. Di Benedetto, R. Carrigan, C. Gatto, S. Geer, C. Johnstone, V.V. Kashikhin, R. Lipton, A. Mazzacane, N. Terentiev and A. Zlobin for collaboration and fruitful discussions.

References

[1] Foster G.W., Mokhov N.V. Backgrounds and Detector Performance at a 2x2 TeV $\mu^+\mu^-$ Collider, *AIP Conf. Proc.* **352**, Sausalito (1994), pp. 178-190.

[2] Johnstone C.J., Mokhov N.V. Optimization of a muon collider interaction region with respect to detector backgrounds and the heat load to the cryogenic systems. In *Proc. Snowmass 1996*, pp. 226-229 (1996).

[3] Johnstone C.J., Mokhov N.V. Shielding the Muon Collider Interaction Region. In *Proc. PAC97*, pp. 414-416 (1997).

[4] Ankenbrandt C. et al. Status of muon collider research and development and future plans. *Phys.Rev.ST Accel.Beams* **2** (1999) 081001

[5] Alexahin Y.I., Gianfelice-Wendt E., Kashikhin V.V., Mokhov N.V., Zlobin A.V, Alexakhin V.Y. Muon Collider Interaction Region Design. *Phys.Rev.ST Accel.Beams* **14**:061001, 2011.

[6] Mokhov N.V., Alexahin Y.I., Kashikhin V.V., Striganov S.I., Zlobin A.V. Muon Collider Interaction Region and Machine-Detector Interface Design. Fermilab-Conf-094-APC-TD (2011), MOODN6 paper at PAC2011.

[7] Mokhov N.V., The Mars Code System User's Guide, Fermilab-FN-628 (1995); Mokhov N.V., Striganov S.I. MARS15 Overview, *Proc. of Hadronic Shower Simulation Workshop*, Fermilab, September 2006, *AIP Conf. Proc.* **896**, pp. 50-60 (2007).

[8] http://www.4thconcept.org/4LoI.pdf

[9] Terentiev N.K., Di Benedetto V., Gatto C., Mazzacane A., Mokhov N.V., Striganov S.I. ILCRoot tracker and vertex detector response to MARS15 simulated backgrounds in the muon collider. *TIPP2011 Conference Proceedings.*